



Published in final edited form as:

Ophthalmol Retina. 2020 October ; 4(10): 1008–1015. doi:10.1016/j.oret.2020.03.027.

Vitreous Findings by Handheld Spectral Domain Optical Coherence Tomography Correlate with Retinopathy of Prematurity Severity

Alex T. Legocki, MD¹, Emily M. Zepeda, MD¹, Thomas B. Gillette, MD¹, Laura E. Grant, MD¹, Ayesha Shariff, MD¹, Phanith Touch, BS¹, Aaron Y. Lee, MD, MSCI¹, Leona Ding, MS¹, Marcela M. Estrada, MD¹, Kristina Tarczy-Hornoch, MD, DPhil^{1,2}, Cecilia S. Lee, MD, MS¹, Dennis E. Mayock, MD^{3,4}, Kathryn L. Pepple, MD, PhD¹, Michelle T. Cabrera, MD^{1,2}

¹Department of Ophthalmology, University of Washington, Seattle, WA, USA

²Department of Ophthalmology, Seattle Children's Hospital, Seattle, WA, USA

³Department of Pediatrics, University of Washington, Seattle, WA, USA

⁴Department of Pediatrics, Seattle Children's Hospital, Seattle, WA, USA

Abstract

Objective: To evaluate the association between retinopathy of prematurity and vitreous findings in premature infants detected by handheld spectral-domain optical coherence tomography.

Design: Prospective, observational cohort study.

Participants: Consecutive sample of 92 premature infants requiring retinopathy of prematurity screening at two academic neonatal intensive care units, between July 2015 and March 2018.

Methods: Infants underwent handheld spectral domain optical coherence tomography at the time of routine retinopathy of prematurity examinations. Two masked, trained graders analyzed right eye vitreoretinal findings including semi-automated quantification of punctate hyperreflective vitreous opacities within 5 foveal/parafoveal B-scans (Vitreous Opacity Ratio).

Main Outcome Measures: Excluding post-treatment data, vitreous findings were compared to clinical retinopathy of prematurity diagnoses.

Results: Agreement between image graders for all vitreoretinal findings was 91% (kappa=0.86 [95% confidence interval, 0.82–0.90], P<0.001). Among 92 infants undergoing 280 imaging sessions (52% male, mean gestational age 28.3±2.8 weeks, mean birthweight 1014.5±285.0 grams), 36/92 (39%) developed retinopathy of prematurity. Punctate hyperreflective vitreous opacities were identified in 61/92 (66%) infants. The presence of punctate hyperreflective vitreous opacities at least once was associated with a diagnosis of retinopathy of prematurity (62% vs. 29% without opacities, P=0.003), maximum retinopathy of prematurity stage (P=0.001), pre-plus or plus disease (24% vs. 5%, P=0.005), and type 1 disease (14% vs. 2%, P=0.03). Among 29 infants

Corresponding author and address for reprints: Michelle T. Cabrera, MD, OA.9.220, 4800 Sand Point Way NE, Seattle, WA 98105, cabreram@uw.edu, Phone: 206-987-3670; Fax: 206-987-3925.

No conflicting relationship exists for any author.

(45 imaging sessions) with right eye punctate hyperreflective vitreous opacities, the Vitreous Opacity Ratio from two graders (F1 score 0.82 ± 0.36 , Dice coefficient 0.97 ± 0.04) correlated with retinopathy of prematurity stage ($P=0.02$). Tractional vitreous bands on imaging correlated with plus disease status (29% vs. 5% without bands, $P=0.05$).

Conclusions: Punctate hyperreflective vitreous opacities and tractional vitreous bands predict the presence and severity of retinopathy of prematurity. Further studies should explore handheld optical coherence tomography as a non-invasive retinopathy of prematurity screening tool.

Retinopathy of prematurity (ROP) remains a leading cause of childhood blindness in the United States and an emerging epidemic in middle-income countries worldwide.¹ While retinal pathology identified during screening eye examinations has been closely linked to risk of ROP blindness and need for preventive treatment,² the role of the vitreous in ROP progression is poorly understood.

Handheld spectral domain optical coherence tomography (SD-OCT) is an excellent tool for longitudinal studies of the retina in awake preterm infants. OCT in these infants has identified numerous retinal pathologies including epiretinal membrane (ERM), cystoid macular edema (CME), retinoschisis, and the ROP ridge.³⁻⁸ *Maldonado et al.* identified four additional plus disease-associated handheld SD-OCT findings in infants with severe ROP (elevated retinal vessels, scalloped retina, hyporefective vessel lumen, and retinal spaces).⁹

We previously described both punctate hyperreflective vitreous opacities and vitreous bands identified by handheld SD-OCT in premature infants screened for ROP.¹⁰ Vitreous bands correlated with both CME and ERM, suggesting a tractional pathophysiology to these entities. This study seeks to further characterize vitreous findings to understand their potential relationship to ROP pathophysiology and OCT-based diagnosis of ROP.

Methods

Study participants

This prospective, observational cohort study recruited premature infants at risk for ROP to undergo handheld SD-OCT imaging at the time of their routine ROP examinations between July 2015 and March 2018. The included subjects overlapped with a previous publication by the authors in 2018.¹⁰ Institutional Review Board approval was obtained at Seattle Children's Hospital and the University of Washington Medical Center. Research adhered to the tenets of the Declaration of Helsinki and the Health Insurance Portability and Accountability Act of 1996. Written informed consent was obtained from all participating infants' legal guardians. Study participants were considered eligible if they required routine ROP screening based on existing criteria (<30 weeks gestation, <1500 grams birth weight, or <2000 grams birth weight with cardiorespiratory instability). Infants deemed too medically unstable for OCT imaging and/or examination were excluded. Standard pupillary dilation with Cyclomydril (phenylephrine hydrochloride 1% and cyclopentolate 0.2%; Alcon Laboratories, Fort Worth, Texas) was performed on all participating infants. Infant demographic data was obtained from the medical record.

ROP diagnosis

One of three pediatric ophthalmologists performed the routine clinical examination using indirect ophthalmoscopy with an eyelid speculum and scleral depression while masked to the OCT findings obtained on the same day. Standard ROP screening and treatment guidelines drove clinical decisions independently of OCT findings.¹¹

Imaging procedure

One of three trained imagers (AS, LEG, and TBG) used a handheld SD-OCT (Envisu C2300; Leica Microsystems, Buffalo Grove, IL) to obtain multiple volumes (100 B-scans per volume) to capture at least one high-quality foveal and optic nerve image in un-sedated, supine infants as described by *Maldonado et al.*¹² Sucrose solution or a pacifier was sometimes required to soothe infants during imaging, but an eyelid speculum was not necessary. Each time an enrolled infant required a routine ROP examination, OCT imaging was performed on the same day.

Grading SD-OCT vitreoretinal findings

Two of three trained graders (AS or TBG and EMZ) used EnvivoVue software (Leica Microsystems, Buffalo Grove, IL) to evaluate all OCT volumes for CME, ERM, vitreous bands, and punctate hyperreflective vitreous opacities. Graders were masked to the clinical ROP screening results and each other's grading. CME was defined as intraretinal hyporeflective spaces distorting retinal layers and visible in more than one B-scan. ERM was defined as a vitreoretinal linear hyperreflective opacity with adjacent hyporeflectivity separating it from the retinal surface, excluding artifact overlying retinal vessels. Punctate hyperreflective opacities had higher signal compared to background, excluding the area above the optic nerve where persistent fetal vasculature remnants are seen. Vitreous bands were defined as hyperreflective linear opacities parallel to the retina (non-tractional) or connecting to the retinal surface (tractional), visible in at least 3 consecutive frames.¹⁰ We further subcategorized vitreous bands as light (thin with lower hyperreflectivity) and dense (thick with higher hyperreflectivity). Disagreement between the two graders was mediated by a third, trained grader (MTC) masked to prior grades.

Quantification of punctate hyperreflective vitreous opacities

To assess whether punctate hyperreflective vitreous opacity density correlated with ROP severity at specific time points, the number of opacities in a uniform segment was determined using semi-automated methods (Figure 1). A subset of non-treated eyes with high-quality images of opacities were analyzed through a custom, open-sourced web browser-based application (<https://github.com/uw-biomedical-ml/segmentations>) developed by one of the authors (AYL). Each completed segmentation was reviewed by an independent trained grader (PT), and inaccurate segmentations were sent back for re-segmentation. The Vitreous Opacity Ratio accounted for the variable size of the vitreous in order to maximize vitreous sampling among five adjacent foveal/parafoveal B-scans (approximate width: 256 microns), excluding the region above the optic nerve. The ratio was defined as total punctate opacities divided by total vitreous area in pixels and averaged between two graders (TBG and MTC).

Statistical analysis

Because treatment substantially increased the number of vitreous opacities, all post-treatment data was excluded. Infants who had ever developed punctate hyperreflective vitreous opacities in either eye were compared to those who had not for demographic and systemic characteristics. Including only right eyes, infants who had ever developed punctate opacities were compared to those who had not for presence of clinically-determined ROP, type 1 ROP,² worst ROP stage, worst plus disease status, and other OCT findings at any time point. To control for postmenstrual age (a potential confounder), a multivariate analysis using a generalized linear mixed model approach was used. Similarly, logistic regression determined whether intraventricular hemorrhage was an independent risk factor for punctate opacities. The maximum Vitreous Opacity Ratio among all imaging sessions was correlated to demographic and systemic characteristics. The Vitreous Opacity Ratio, punctate opacities, and bands were also correlated with clinical ROP and OCT findings at each eye's imaging date.

Birth weight and gestational age failed the Shapiro-Wilk test of normality; therefore, the Mann-Whitney U test was used. All categorical data underwent the Chi-squared test or Fisher's exact test. The unweighted Cohen's kappa (k) statistic assessed intergrader agreement. An F1 score for counting opacities and a Dice coefficient for segmenting vitreous area determined intergrader agreement for the Vitreous Opacity Ratio. A generalized linear mixed model accounted for non-independence of multiple observations per infant. Statistical analyses were performed using SAS version 9.4 (SAS institute, Inc., Cary, NC, USA) and IBM SPSS Statistics for Windows, Version 26.0 (IBM Corp., Armonk, NY). A value of P 0.05 was considered statistically significant.

Results

Subject characteristics

A total of 111 premature infants were recruited. Of these, 19 were excluded (8 were withdrawn due to parental concern for infant stress, 2 were hemodynamically unstable, 2 guardians declined follow-up visits, 1 died from respiratory failure, 5 had lost data, and 1 underwent all imaging sessions after ROP treatment). Among the remaining 92 infants included, 48/92 (52%) were male with mean birth weight 1014.5 (\pm 285.0) grams and mean gestational age 28.3 (\pm 2.8) weeks. Race and ethnicity were assessed due to prior associations with ROP and OCT characteristics (Table 1).^{13,14} By right eye indirect ophthalmoscopy, 36/92 (39%) infants developed ROP and 5/92 (5%) developed type 1 ROP requiring laser treatment. One infant (1%) was treated with laser for stage 3, zone 2, pre-plus disease. The worst ROP stage was stage 3, diagnosed in 13/92 (14%) infants.

Punctate hyperreflective vitreous opacities

A total of 301 imaging sessions were obtained with mean 3 (\pm 2) imaging sessions per infant over 6.0 (\pm 4.8) weeks. Two trained OCT graders had 274/301 (91%) agreement and a kappa score of 0.86 (95% confidence interval [CI], 0.82–0.90). Five imaging sessions missing data and 16 post-treatment imaging sessions were excluded. The remaining 280 imaging sessions of 92 infants were analyzed. Punctate hyperreflective vitreous opacities were seen in one or

both eyes of 61/92 (66%) premature infants and were bilateral in 18/92 (20%) infants. Demographics and comorbidities are shown in Table 1. Infants who had ever had punctate opacities in one or both eyes tended to also have intraventricular hemorrhage (Odds ratio=6.60, 95% CI, 0.81–53.70; P=0.05). However, logistic regression demonstrated no such association when controlling for ROP stage (P=0.87). No other demographic characteristics, systemic comorbidities, or number of comorbidities were associated with punctate opacities. We went on to analyze right eye ocular characteristics. There were 29/92 (32%) right eyes found to have punctate hyperreflective vitreous opacities. They were first detected at mean postmenstrual age 37.6 (\pm 4.6) weeks, after which 12/29 (41%) infants continued to demonstrate their presence throughout all subsequent visits, 13/29 (45%) resolved during the study, and 4/29 (14%) appeared and resolved more than once.

Comparisons between eyes with and without punctate hyperreflective vitreous opacities are shown in Table 2. ROP was clinically diagnosed in 18/29 (62%) right eyes that developed punctate opacities at any time, and 18/63 (29%) that did not (Odds ratio=4.09, 95% CI, 1.62–10.35; P=0.003). Development of right eye punctate opacities at any time was associated with worse ROP stage compared to eyes without opacities (P=0.001). More eyes with punctate opacities also developed pre-plus or plus disease compared to those without (P=0.005). Four of 5 infants whose right eyes reached type 1 ROP requiring treatment (laser photocoagulation) also had punctate opacities detected at some point before treatment. Type 1 ROP was seen more frequently in eyes with punctate opacities than eyes without (P=0.03). Opacities were significantly associated with ERM by OCT at any time (P=0.05). However, opacities were not associated with CME (P=0.81) or vitreous bands (P=0.14) on OCT, nor did they correlate with hemorrhage or vitreous haze by indirect ophthalmoscopy in that eye at any time (P=0.12).

Punctate hyperreflective vitreous opacities and associated ocular findings at each visit

Analyzing individual right eye imaging sessions, punctate opacities were associated with a clinical diagnosis of ROP (P=0.02) and severity of ROP stage (P=0.02). Punctate opacities were also associated with ERM (P=0.003) and tractional vitreous bands (P=0.02). There was no association between punctate opacities and postmenstrual age at time of imaging (P=0.13). Furthermore, secondary multivariate analysis with a generalized linear mixed model demonstrated that ROP stage was an independent risk factor for punctate opacities, controlling for postmenstrual age (P=0.02).

Quantification of punctate hyperreflective vitreous opacities at each visit

Agreement between two graders counting opacities revealed an F1 score of 0.82 [\pm 0.36]. The Dice coefficient for segmenting the vitreous was 0.97 [\pm 0.04]. Three of 4 infants treated with laser for type 1 ROP with available imaging immediately before and approximately one week after treatment demonstrated a marked increase in punctate opacities (mean Vitreous Opacity Ratio: 0.97×10^{-8} vs. 28.28×10^{-8} , 2430% increase; Figure 2). After excluding post-treatment imaging, the remaining 45 right eye imaging sessions from 29 preterm infants were analyzed for demographic and ocular correlations with Vitreous Opacity Ratio (Table 3, available at <https://www.opthalmologyretina.org/>). An association existed between Vitreous Opacity Ratio and ROP stage (P=0.02, Figure 3a) but not plus disease status

($P=0.46$, Figure 3b). However, there were no examination sessions with either plus or pre-plus disease and without punctate opacities (Figure 3b). Vitreous Opacity Ratio was not associated with CME, ERM, or vitreous bands.

Vitreous bands and associated clinical ROP findings at each visit

To test for a relationship between tractional vitreous bands and ROP severity, we analyzed 280 right eye imaging sessions of 92 infants prior to any treatment. Of these, 7/280 (2.5%) imaging sessions (6/92 [7%] infants) had tractional vitreous bands, with two subtypes: dense in 2/7 (14%) imaging sessions of 1 infant and light in 5/7 (86%) imaging sessions of 5 infants. There were no tractional bands that distorted the retina. We identified more pre-plus or plus disease with tractional vitreous bands compared to without ($P=0.05$). No relationship was seen between tractional vitreous bands and ROP stage ($P=0.63$), presence of ROP ($P=0.50$), or type 1 ROP ($P=0.12$). No association was found between non-tractional vitreous bands and ROP, ROP stage, plus disease status, or type 1 ROP.

There were 32 cases of disagreement between the two graders among 27/301 (9%) imaging sessions; 14/32 (44%) were due to disagreement on the presence of ERM vs. normal hyperreflective nerve fiber layer, 11/32 (34%) on subtle intraretinal cysts vs. hyporeflexive artifact in darker scans, 4/32 (13%) on vitreous bands vs. hyperreflective artifact, and 3/32 (9%) on presence of punctate opacities vs. artifact.

Discussion

This study identified an association between presence of punctate hyperreflective vitreous opacities seen on handheld SD-OCT and ROP development ($p=0.003$) and severity (worst ROP stage: $P=0.001$; worst plus disease status: $P=0.005$; Type 1 ROP: $P=0.03$) among 92 preterm infants screened for ROP. This association was also present for individual imaging sessions when controlling for postmenstrual age (ROP stage: $P=0.02$) and existed prior to any treatment for ROP. The correlation with ROP stage was particularly evident in a sub-analysis quantifying the punctate hyperreflective vitreous opacities in and around the fovea ($P=0.02$). Although the presence of punctate hyperreflective vitreous opacities on a handheld OCT screening examination does not predict whether a child will develop ROP, this study determined that it is a significant risk factor (OR 4.09).

It is unknown what punctate hyperreflective vitreous opacities seen on OCT represent in premature infants at risk for ROP, but they are not always related to ROP. Despite the strong associations noted, 38% of infant eyes with punctate hyperreflective vitreous opacities did not develop ROP. Proteomic analysis of the vitreous of infants with ROP has identified many proteins not present in control patients undergoing congenital cataract extraction, although only vascular endothelial growth factor (VEGF) was consistently present in active ROP compared to inactive ROP.¹⁵⁻²¹ Alternatively, punctate hyperreflective vitreous opacities may represent inflammatory cells. Inflammatory markers have been isolated in the vitreous of infants with ROP, and macrophages/microglia were detected in the vitreous of ROP babies under oxidative stress in a cell culture model.^{15,16} Furthermore, we found a prominent increase in the number of punctate hyperreflective vitreous opacities (Vitreous Opacity Ratio) immediately following laser treatment for type 1 ROP, which supports the

inflammatory cell hypothesis since laser retinal photocoagulation is known to increase inflammation.^{17,18} The link between the number of punctate hyperreflective vitreous opacities (Vitreous Opacity Ratio) and ROP stage supports the hypothesis that punctate hyperreflective vitreous opacities seen by OCT may also represent retinal astrocyte precursors or hemoglobin released from the stage 2 or 3 ridge.¹⁹ Finally, punctate hyperreflective vitreous opacities may represent a combination of the above entities.

Little is known about vitreous findings in preterm infants by handheld SD-OCT. We previously published on vitreous bands identified by handheld SD-OCT, hypothesizing that tractional bands may lead to tractional retinal detachment in advanced ROP, however no correlations between vitreous bands and punctate hyperreflective vitreous opacities or ROP severity were seen.¹⁰ In the current study, we analyzed images at a more granular level, assessing OCT and clinical findings at specific visits in that eye. With this approach, tractional vitreous bands correlated with plus disease status ($P=0.05$), in spite of a small sample size of plus disease. Based on this study, tractional vitreous bands and punctate hyperreflective vitreous opacities are potential markers of ROP severity.

While current standard screening examinations are effective in identifying high risk infants who require intervention to prevent blindness,¹¹ these screening examinations lead to significant systemic morbidity and distress for these fragile infants. Binocular indirect ophthalmoscopy and wide-field retinal photography both involve direct ocular contact and the use of an eyelid speculum eliciting significant increases in pain scores and cardiorespiratory instability.²⁰⁻²⁴ In contrast, handheld OCT is a non-contact modality that does not require an eyelid speculum. By identifying two potential new OCT markers for ROP severity risk in addition to previously identified OCT markers,⁹ this study opens up the possibility for exploration of handheld OCT as a safer diagnostic tool than currently accepted ROP screening methods.

This study is limited by its observational design. Nonetheless, we had high interobserver agreement. The quantification of punctate hyperreflective vitreous opacities was also limited to the foveal and parafoveal region of the eye, thereby potentially missing opacities visible elsewhere. Furthermore, opacity distribution relative to distance above the retina may not be uniform, leading to uneven capture of opacities in images of variable depth. Special attention to the vitreous surrounding the ROP ridge, for example, may reveal particularly high numbers of punctate hyperreflective vitreous opacities if these opacities originate there. However, foveal and parafoveal images were felt to provide representative sampling with high image quality and uniform anatomic localization. Future studies should explore wide field handheld OCT along with automated software to analyze the entire vitreous volume.

In summary, this study identifies two potential new markers predictive of ROP development and severity based on awake handheld SD-OCT imaging of at-risk premature infants: punctate hyperreflective vitreous opacities and tractional vitreous bands. Future studies should incorporate multiple known OCT ROP predictors to explore handheld OCT as a potential ROP screening tool.

Acknowledgments

The authors would like to acknowledge Nicole Mattson, Luke Johnson, Calvin Lee, Jordan Sandhu (all University of Washington undergraduate student volunteers), and Hannah Walsh (Yale undergraduate student volunteer) for serving as research assistants for this study.

Financial Support:

This work is supported by The Knights Templar Eye Foundation (MTC), the Latham Vision Research Innovation Award (MTC), NIH K23EY029246 (AYL), and unrestricted grants from Research to Prevent Blindness and the NIH CORE Grant EY001730.

The funding organizations had no role in the design or conduct of this research.

Abbreviations:

ROP	retinopathy of prematurity
SD-OCT	spectral-domain optical coherence tomography
ERM	epiretinal membrane
CME	cystoid macular edema
CI	confidence interval
VEGF	vascular endothelial growth factor

References

1. Solebo AL, Teoh L, Rahi J. Epidemiology of blindness in children. *Arch Dis Child*. 2017;102(9):853–857. [PubMed: 28465303]
2. Good WV, Early Treatment for Retinopathy of Prematurity Cooperative G. Final results of the Early Treatment for Retinopathy of Prematurity (ETROP) randomized trial. *Trans Am Ophthalmol Soc*. 2004;102:233–248; discussion 248–250. [PubMed: 15747762]
3. Lee AC, Maldonado RS, Sarin N, O’Connell RV, Wallace DK, Freedman SF, Cotten M, Stinnett SS, Toth CA. Spectral Domain Optical Coherence Tomography as an Adjunct to Indirect Ophthalmoscopy for Retinopathy of Prematurity. *Retina*. 2011 In press.
4. Chavala SH, Farsiou S, Maldonado R, Wallace DK, Freedman SF, Toth CA. Insights into advanced retinopathy of prematurity using handheld spectral domain optical coherence tomography imaging. *Ophthalmology*. 2009;116(12):2448–2456. [PubMed: 19766317]
5. Muni RH, Kohly RP, Charonis AC, Lee TC. Retinoschisis detected with handheld spectral-domain optical coherence tomography in neonates with advanced retinopathy of prematurity. *Arch Ophthalmol*. 2010;128(1):57–62. [PubMed: 20065217]
6. Dubis AM, Subramaniam CD, Godara P, Carroll J, Costakos DM. Subclinical macular findings in infants screened for retinopathy of prematurity with spectral-domain optical coherence tomography. *Ophthalmology*. 2013;120(8):1665–1671. [PubMed: 23672969]
7. Vinekar A, Avadhani K, Sivakumar M, et al. Understanding clinically undetected macular changes in early retinopathy of prematurity on spectral domain optical coherence tomography. *Investigative ophthalmology & visual science*. 2011;52(8):5183–5188. [PubMed: 21551410]
8. Bondalapati S, Milam RW Jr., Ulrich JN, Cabrera MT. The Characteristics and Short-term Refractive Error Outcomes of Cystoid Macular Edema in Premature Neonates as Detected by Spectral-Domain Optical Coherence Tomography. *Ophthalmic surgery, lasers & imaging retina*. 2015;46(8):806–812.

9. Maldonado RS, Yuan E, Tran-Viet D, et al. Three-dimensional assessment of vascular and perivascular characteristics in subjects with retinopathy of prematurity. *Ophthalmology*. 2014;121(6):1289–1296. [PubMed: 24461542]
10. Zepeda EM, Shariff A, Gillette TB, et al. Vitreous Bands Identified by Handheld Spectral-Domain Optical Coherence Tomography Among Premature Infants. *JAMA ophthalmology*. 2018;136(7):753–758. [PubMed: 29799932]
11. Fierson WM, Ophthalmology AAOPSo, American Academy Of O, American Association For Pediatric O, Strabismus, American Association Of Certified O. Screening Examination of Premature Infants for Retinopathy of Prematurity. *Pediatrics*. 2018;142(6).
12. Maldonado RS, Izatt JA, Sarin N, et al. Optimizing hand-held spectral domain optical coherence tomography imaging for neonates, infants, and children. *Invest Ophthalmol Vis Sci*. 2010;51(5):2678–2685. [PubMed: 20071674]
13. Cabrera MT, O’Connell RV, Toth CA, et al. Macular findings in healthy full-term Hispanic newborns observed by hand-held spectral-domain optical coherence tomography. *Ophthalmic surgery, lasers & imaging retina*. 2013;44(5):448–454.
14. Saunders RA, Donahue ML, Christmann LM, et al. Racial variation in retinopathy of prematurity. The Cryotherapy for Retinopathy of Prematurity Cooperative Group. *Arch Ophthalmol*. 1997;115(5):604–608. [PubMed: 9152127]
15. Sato T, Kusaka S, Shimojo H, Fujikado T. Simultaneous analyses of vitreous levels of 27 cytokines in eyes with retinopathy of prematurity. *Ophthalmology*. 2009;116(11):2165–2169. [PubMed: 19700197]
16. Rathi S, Jalali S, Patnaik S, et al. Abnormal Complement Activation and Inflammation in the Pathogenesis of Retinopathy of Prematurity. *Front Immunol*. 2017;8:1868. [PubMed: 29312345]
17. Nonaka A, Kiryu J, Tsujikawa A, et al. Inflammatory response after scatter laser photocoagulation in nonphotocoagulated retina. *Invest Ophthalmol Vis Sci*. 2002;43(4):1204–1209. [PubMed: 11923267]
18. Richardson PR, Boulton ME, Duvall-Young J, McLeod D. Immunocytochemical study of retinal diode laser photocoagulation in the rat. *Br J Ophthalmol*. 1996;80(12):1092–1098. [PubMed: 9059277]
19. Sun Y, Dalal R, Gariano RF. Cellular composition of the ridge in retinopathy of prematurity. *Arch Ophthalmol*. 2010;128(5):638–641. [PubMed: 20457991]
20. Mukherjee AN, Watts P, Al-Madfai H, Manoj B, Roberts D. Impact of retinopathy of prematurity screening examination on cardiorespiratory indices: a comparison of indirect ophthalmoscopy and retcam imaging. *Ophthalmology*. 2006;113(9):1547–1552. [PubMed: 16828505]
21. Mehta M, Adams GG, Bunce C, Xing W, Hill M. Pilot study of the systemic effects of three different screening methods used for retinopathy of prematurity. *Early Hum Dev*. 2005;81(4):355–360. [PubMed: 15814220]
22. Moral-Pumarega MT, Caserio-Carbonero S, De-La-Cruz-Bertolo J, Tejada-Palacios P, Lora-Pablos D, Pallas-Alonso CR. Pain and stress assessment after retinopathy of prematurity screening examination: indirect ophthalmoscopy versus digital retinal imaging. *BMC Pediatr*. 2012;12:132. [PubMed: 22928523]
23. Rush R, Rush S, Nicolau J, Chapman K, Naqvi M. Systemic manifestations in response to mydriasis and physical examination during screening for retinopathy of prematurity. *Retina*. 2004;24(2):242–245. [PubMed: 15097885]
24. Laws DE, Morton C, Weindling M, Clark D. Systemic effects of screening for retinopathy of prematurity. *Br J Ophthalmol*. 1996;80(5):425–428. [PubMed: 8695564]

Punctate hyperreflective vitreous opacities and tractional vitreous bands, as seen by handheld optical coherence tomography, were associated with the presence and severity of retinopathy of prematurity in premature infants.

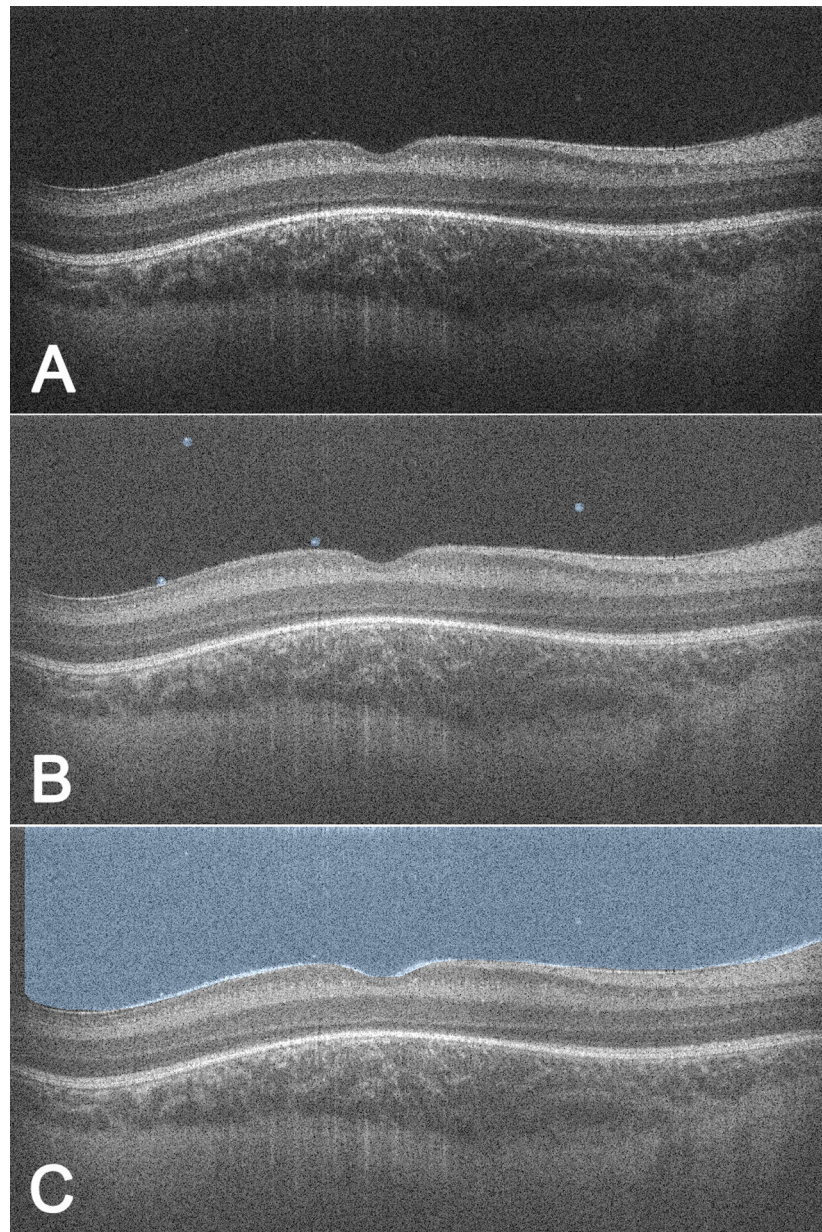


Figure 1. Semi-automated quantification of punctate hyperreflective vitreous opacities to determine Vitreous Opacity Ratio. For each right eye imaging session, each of five (A) B-scans centered on the fovea (total width ~256 microns) were analyzed by two trained graders through a custom web-based application to (B) manually circle punctate hyperreflective vitreous opacities to allow for computer counting of opacities and (C) manually demarcate the inner retinal border to allow for computer segmentation of the total vitreous area above the border. The VOR was calculated as the total number of punctate hyperreflective vitreous opacities among all five B-scans divided by the total visible vitreous area in pixels and averaged between the two graders. VOR = Vitreous Opacity Ratio.

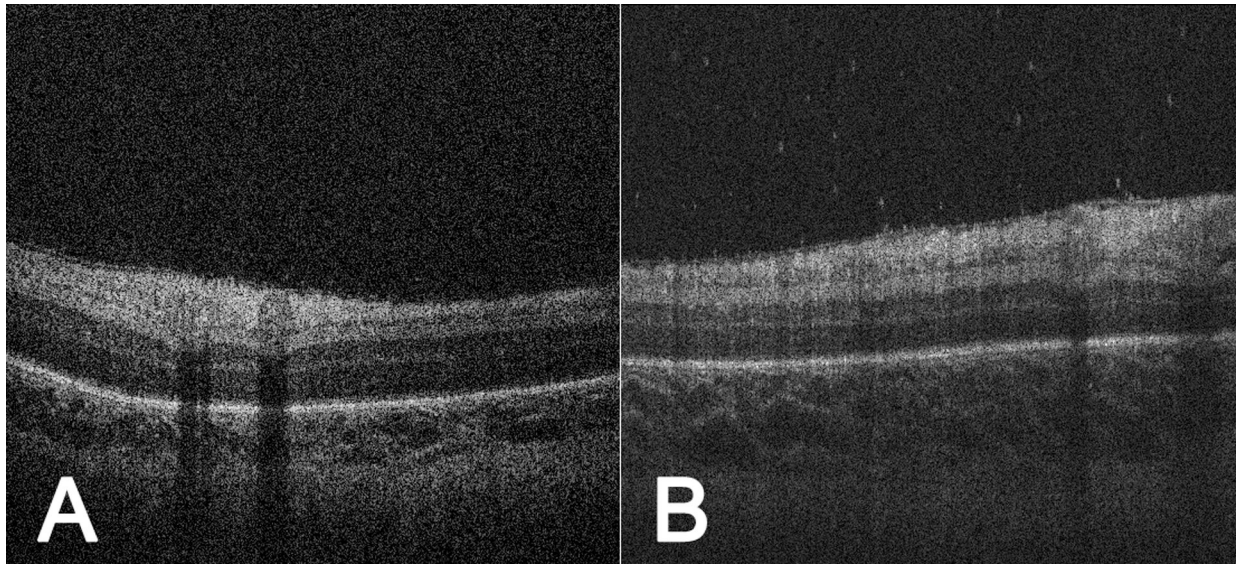


Figure 2.

Punctate hyperreflective vitreous opacities increased following retinal laser photocoagulation. Handheld SD-OCT images of the right eye of a premature infant (birth weight 729.0 grams, gestational age 25.0 weeks) at (A) postmenstrual age 38.4 weeks, just prior to retinal laser photocoagulation for type 1 ROP, $VOR = 1.05 \times 10^{-8}$, and at (B) postmenstrual age 39.4 weeks, one week following retinal laser photocoagulation, $VOR = 53.61 \times 10^{-8}$. We found that 3/4 infants treated with laser retinal photocoagulation for type 1 ROP demonstrated a marked increase in VOR (mean pre-laser vs. post-laser VOR: 0.97×10^{-8} vs. 28.28×10^{-8} , 2430% increase). As a side note, both images here demonstrate an epiretinal membrane, which was associated with punctate hyperreflective vitreous opacities ($P=0.003$ among all right eye imaging sessions). SD-OCT = spectral domain optical coherence tomography; ROP = retinopathy of prematurity; VOR = Vitreous Opacity Ratio.

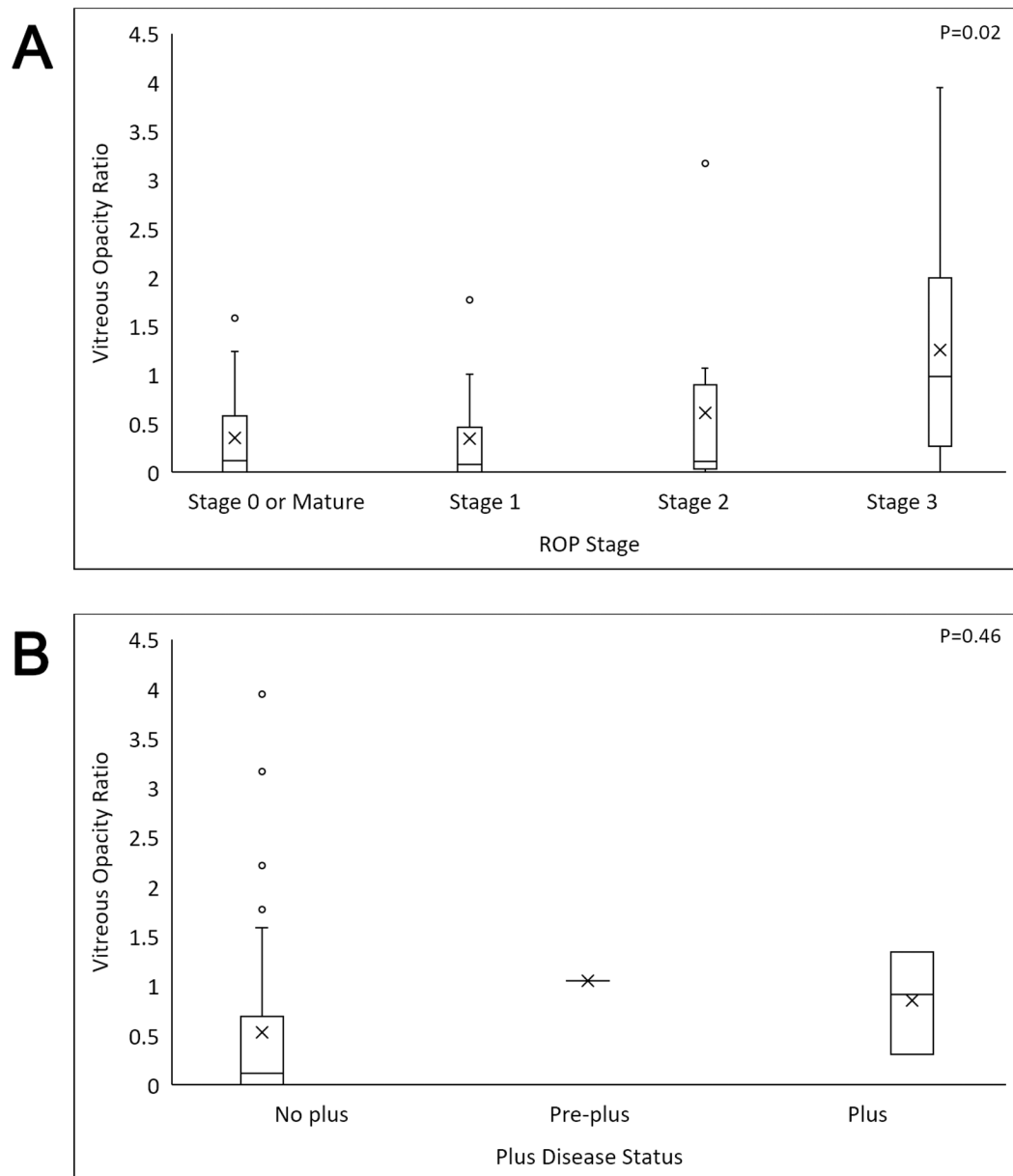


Figure 3. Quantified punctate hyperreflective vitreous opacities (VOR) correlated with ROP severity. Box and whisker plots of the VOR (center lines = medians, X's = means, boxes = quartiles, whiskers = ranges, open circles = outliers). A significant association was found between VOR and (A) ROP stage ($P=0.02$). Although there was no significant association between VOR and (B) plus disease status ($P=0.46$), there were no cases of pre-plus or plus disease in the absence of punctate hyperreflective vitreous opacities. ROP = retinopathy of prematurity; VOR = Vitreous Opacity Ratio.

Table 1.

Comparison between Premature Infants with and without Punctate Hyperreflective Vitreous Opacities in Either Eye for Demographics and Patient Comorbidities

Characteristic	No Punctate Hyperreflective Vitreous Opacities No. (%) of Infants n = 31 ^a	Presence of Punctate Hyperreflective Vitreous Opacities n = 61 ^b	P-value ^c
Demographics			
Male	18 (58)	30 (49)	0.51
Birth weight, mean (SD), grams	1043.3 (239.3)	999.9 (306.4)	0.21
Gestational age, mean (SD), weeks	28.8 (2.2)	28.1 (3.1)	0.46
Race / ethnicity			
White	21 (68)	33 (54)	0.29
Hispanic	4 (13)	12 (20)	
Native American	1 (3)	2 (3)	
Black	0 (0)	4 (7)	
Asian	2 (7)	3 (5)	
Pacific Islander	1 (3)	0 (0)	
Other ^d	2 (7)	7 (12)	
Comorbidities			
Associated respiratory disease	19 (61)	32 (53)	0.51
Heart defect	7 (23)	18 (30)	0.62
Sepsis	3 (10)	8 (13)	0.75
Bronchopulmonary dysplasia	4 (13)	10 (16)	0.77
Intraventricular hemorrhage	1 (3)	11 (18)	0.05
Anemia	8 (26)	13 (21)	0.61
Anemia requiring transfusion	1 (3)	7 (12)	0.26

SD = standard deviation.

^aNo punctate opacities in either eye.

^bPunctate opacities present in one or both eyes.

^cAll categorical data were analyzed by Fisher's Exact test or Chi-Square test. Continuous data were analyzed by Non-Parametric Mann-Whitney U for two sample test.

^dPatients who did not have a race/ethnicity listed in their medical records.

Table 2.

Comparison between Right Eyes with Punctate Hyperreflective Vitreous Opacities and Those Without Punctate Hyperreflective Vitreous Opacities for Ocular Characteristics Prior to Treatment

Characteristic	No Punctate Hyperreflective Vitreous Opacities n = 63	Presence of Punctate Hyperreflective Vitreous Opacities n = 29	P-value ^a
Indirect ophthalmoscopic examination findings			
Diagnosis of ROP	18 (29)	18 (62)	0.003
Maximum stage of ROP			
ROP stage 0	45 (71)	11 (38)	0.001
ROP stage 1	9 (14)	5 (17)	
ROP stage 2	4 (6)	5 (17)	
ROP stage 3	5 (8)	8 (28)	
Presence of pre-plus or plus disease	3 (5)	7 (24)	0.005
Type 1 ROP	1 (2)	4 (14)	0.03
Hemorrhage or vitreous haze	2 (3)	4 (14)	0.12
SD-OCT findings			
Cystoid macular edema	19 (30)	10 (35)	0.81
Epiretinal membrane	14 (22)	13 (45)	0.05
Vitreous bands	14 (22)	11 (38)	0.14
Tractional subtype	2 (3)	3 (10)	0.32
Non-tractional subtype	14 (22)	9 (31)	0.44

SD = standard deviation; ROP = retinopathy of prematurity; SD-OCT = spectral domain optical coherence tomography.

^aAll Categorical data were analyzed by Fisher's Exact test or Chi-Square test. Continuous data were analyzed by Non-Parametric Mann-Whitney U for two sample test.

Table 3.

Vitreous Opacity Ratio (Quantified Punctate Hyperreflective Vitreous Opacities) and its Relationship with Demographic and Ocular Characteristics in a Subset of Premature Infants

Characteristic, n = 29	Vitreous Opacity Ratio, mean (SD) ^a	P-value
Patient Characteristics^b		
Demographics		
Gender		0.65
Male	0.79 (1.14)	
Female	0.61 (0.93)	
Birth weight		0.51 ^c
<800 grams	0.85 (1.15)	
800 grams	0.53 (0.87)	
Gestational age		0.23 ^c
<26 weeks	1.07 (1.25)	
26 weeks	0.46 (0.79)	
Race / Ethnicity		0.42
White	0.40 (0.86)	
Hispanic	0.51 (0.58)	
American Indian	0.66 (0.29)	
Black	0.94 (0.91)	
Asian	1.62 (2.07)	
Other ^d	1.33 (1.17)	
Ocular Characteristics^e		
Indirect ophthalmoscopic examination findings		
Presence of ROP		0.19
Absent	0.36 (0.47)	
Present	0.70 (1.02)	
Stage of ROP		0.02
ROP stage 0	0.35 (0.48)	
ROP stage 1	0.34 (0.56)	
ROP stage 2	0.61 (1.03)	
ROP stage 3	1.25 (1.30)	
Plus disease status		0.46
No plus disease	0.53 (0.88)	
Pre-plus disease	1.05 (0.00)	
Plus disease	0.85 (0.52)	
Type 1 ROP		0.41
Absent	0.53 (0.88)	
Present	0.90 (0.44)	
SD-OCT findings		

Characteristic, n = 29	Vitreous Opacity Ratio, mean (SD) ^a	P-value
Cystoid macular edema		0.57
Absent	0.52 (0.83)	
Present	0.70 (0.97)	
Epiretinal membrane		0.07
Absent	0.34 (0.58)	
Present	0.80 (1.03)	
Non-tractional vitreous bands		0.87
Absent	0.57 (0.91)	
Present	0.51 (0.48)	
Tractional vitreous bands		0.85
Absent	0.55 (0.88)	
Present	0.65 (0.57)	

SD = standard deviation; ROP = retinopathy of prematurity; SD-OCT = spectral domain optical coherence tomography.

^aAll findings are for the right eye only. Analysis was performed on a subset of 45 imaging sessions among 29 infants selected for known punctate hyperreflective vitreous opacities, excluding post-ROP treatment images. Vitreous Opacity Ratio was calculated using a semi-automated process shown in Figure 1. Two graders identified opacities and manually demarcated the inner retinal border within the five B-scans centered on the fovea (total width roughly 256 microns). The Vitreous Opacity Ratio was calculated as the total number of punctate opacities divided by the visible vitreous area in pixels and averaged between the two graders. Vitreous Opacity Ratio is divided by 10^{-8} to display the coefficient only.

^bPatient characteristics were compared using each of the 29 infants' maximum Vitreous Opacity Ratio among all right eye imaging sessions.

^cAnalyses to determine P-values were performed for the continuous variables of birth weight and gestational age rather than the categories listed here.

^dPatients who did not have a race/ethnicity listed in their medical records.

^eRight eye ocular characteristics were correlated to the Vitreous Opacity Ratios at each of the 45 imaging sessions, among 29 infants. A generalized linear mixed model was used to account for non-independence of multiple observations per infant.